MN-CRCN: A NEW BENCHMARK FOR AUTOMATIC MICRONUCLEUS DETECTION IN LYMPHOCYTES

Camile Alheiro Barbosa
Universidade Federal Rural de Pernambuco

RESUMO

A detecção de micronúcleos (MN) em linfócitos binucleados é um importante biomarcador para a avaliação da instabilidade cromossômica e dos efeitos genotóxicos, desempenhando um papel fundamental em diagnósticos relacionados ao câncer e em estudos toxicológicos. No entanto, a análise manual é um processo demorado, subjetivo e suscetível a erros humanos. Os trabalhos encontrados na literatura para detecção de micronúcleos utilizam bases de dados privadas, o que limita a avaliação e a reprodutibilidade dos modelos propostos. Neste trabalho, apresentamos o MN-CRCN, um novo conjunto de dados público composto por 889 imagens de alta resolução de linfócitos binucleados, anotadas por especialistas, contendo a localização tanto das células binucleadas quanto dos micronúcleos. Avaliamos modelos de detecção de objetos do estado da arte, incluindo Faster R-CNN, RetinaNet, FCOS, YOLOv11 e YOLOv12, utilizando as métricas mAP@50, precisão e revocação. Os experimentos realizados no MN-CRCN demonstraram que o YOLOv12 obteve o melhor desempenho, alcançando 93% de precisão, 93% de revocação e 96% de mAP@50. Os resultados evidenciam o potencial dos métodos de aprendizado profundo como ferramenta de apoio à análise citogenética e ressaltam a importância da disponibilização de bases de dados abertas para a avaliação comparativa de métodos automáticos de detecção de micronúcleos.

Palavras-chave: Detecção de objetos, Micronúcleo, Visão Computacional.

Datas de submissão e aprovação do artigo: 01/07/2026

1 INTRODUCTION

Micronuclei (MN) are cellular structures formed by chromo-somal fragments or entire chromosomes that fail to reintegrate into the main nucleus after cell division, remaining in the cyto-plasm as small accessory nuclei [1]. These micronuclei arise due to errors in chromosomal segregation during mitosis or meiosis and are considered important biomarkers for assessing genetic damage and chromosomal instability. Their detection is widely used in genomic toxicology research and significantly contributes to studies on cancer and other diseases related to genetic instability [1].

Traditionally, the detection and counting of micronuclei are performed manually by experienced cytogeneticists, making the process time-consuming, labour-intensive, and prone to interpretation errors. The subjectivity of the assessment, com-bined with the variability in the quality of microscopic images, can lead to inconsistencies between observers, affecting diag-nostic accuracy [2]. Additionally, low-quality images, often obtained through conventional microscopes, can make the identification process even more challenging and imprecise. Therefore, the cytogeneticist's experience and skill play a crucial role in the correct classification of micronuclei, which, however, can make the analysis subjective and susceptible to interpretative biases.

To address this problem, works in the literature apply deep learning models, such as YOLO [3], to identify micronuclei in cytogenetic images [4], [5]. Despite the advances in micronuclei detection, there are still challenges related to the quality of the images, difficult cases to analyze and missings in the detection task. Most of the research with micronuclei images relies on private datasets, making it difficult to reproduce results, analyze models and improve state-of-the-art (SOTA). In this work, we developed a new dataset of lymphocyte images for automatic micronuclei detection tasks. The dataset is composed of images captured at the Centro Regional de Ciências Nucleares do Nordeste (CRCN-NE), which were carefully annotated to ensure accurate identification of the classes. The dataset comprises binucleated cells without micronuclei and binucleated cells with micronuclei, with the respective annotation of localization of cells and micronuclei. To evaluate the dataset, we built a benchmark of SOTA methods object detection, composed by Faster-RCNN [6], FCOS [7], RetinaNet [8], YOLOv11 [3], and YOLOv12 [9].

The main contributions of this work include:

- Construction and public release of a new dataset containing detailed annotations of mononucleated cells, binucleated cells, and micronuclei, aiming to standardize and facilitate the reproducibility of experiments in the field;
- Evaluation of SOTA object detection deep learning models for the micronuclei task;

2 PRIOR WORK

Automated detection of micronuclei (MN) in cellular images has been investigated using deep learning models. Among these approaches, models from the YOLO (You Only Look Once) family [10] have received special attention for their high accuracy and real-time object detection speed. Wei et al. [11] proposed an enhanced version of YOLOv5, named YOLOv5-CEB, which incorporates attention mechanisms to improve micronucleus detection accuracy. Experimental results from this study show a 2% increase in mean precision, a 2% increase in accuracy, and a 1.3% increase in recall compared to the original YOLOv5 algorithm. Modern architectures such as YOLOv12 already include attention mechanisms but have not been tested on micronuclei datasets. Their use uses a private dataset composed of 726 images with micronucleous cells.

Another significant contribution was proposed by Wei et al. [12], who developed STD-YOLOv7, a small-object detector for micronuclei based on the YOLOv7 architecture. This model incorporates the Coordinated Attention mechanism, enhancing micronucleus detection accuracy by allowing the network to focus on critical image regions. Experiments are performed on the SRCHD [12] private dataset, composed of 13,309 images.

Ibarra-Arellano et al. [13] presented micronuclAI, a graphical interface tool for the automated quantification of micronuclei of various sizes, morphologies, and locations. The classifier achieved near-human-level performance using a convolutional neural network trained to analyze cropped images of individual cells from datasets comprising various human and murine cell lines. Although they use public datasets, their approach focuses on the segmentation task.

In addition to these advances, Shen et al. [14] developed an approach for rapid and automated detection of micronuclei in images of binucleated lymphocytes using convolutional neural network (CNN) algorithms. This system was designed to analyze images obtained using automated microscopes, offering an efficient and accessible alternative to the manual and subjective micronucleus counting process.

Their approach achieved a 99.4% detection rate compared to manual detection, with a 14.7% false positive rate on tests conducted with 20 slides. Their experiments are conducted on the private CBMN dataset [14].

Despite progress in the field, the aforementioned works rely on private datasets, limiting the reproducibility of experiments and direct comparison between approaches. Also, the type of image varies depending on the dataset, as the acquisition technique may differ from each laboratory. This also makes it difficult to compare different SOTA techniques. Figure 1 shows the type of images of datasets used in CBMN [14], (b) Wei's dataset [11], (d) NCI-H358 dataset [13], and (d) MN-CRCN (ours). We can observe from Figure 1 that the images from the datasets can vary in terms of luminosity, noise and noisy elements in the image and structure of the cells. The CBMN dataset, shown in Figure 1, has a similar image as ours, which is used in the CRCN laboratory. However, CBMN is a private dataset.

Figure 1 – Example of images from (a) CBMN [14] dataset (private), (b) Wei's dataset [11] (private), NCI-H358 dataset [13] (private), and (d) MN-CRCN (ours, public)

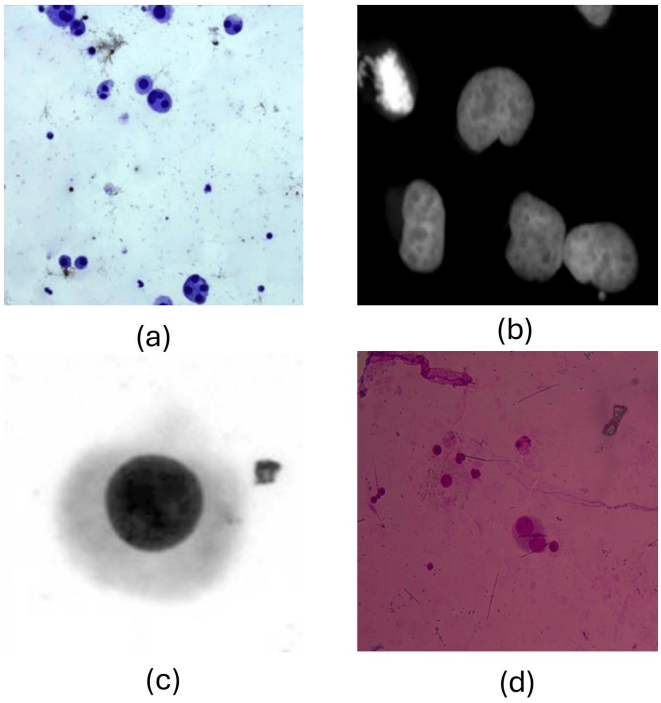

Fonte: Barbosa, 2026.

Based on these limitations, we built our own dataset, called MN-CRCN, containing images collected at CRCN-NE, with annotations of the locations of binucleated cells and micronuclei. By making the dataset publicly available, we aim to standardize model evaluation and promote the reproducibility of experiments in this field. Our work also differs from these approaches by employing the most recent version of YOLO (YOLOv11 and YOLOv12) and extending the analysis for other SOTA object detection.

3 BACKGROUND

The cells obtained from slides of human lymphocyte cultures can be mononucleated and multinucleated cells. Each cell may have a small structure called micronuclei. The cells may vary in size, amount of micronuclei, touching elements, and

nucleoplasmic bridges [15]. The Micronuclei Detection task consists of identifying a micronuclei (MN) in binucleated cells. Figure 2 shows examples of mononucleated cells, binucleated cells without micronuclei and binucleated cells with micronuclei.

Figure 2 – (a) Mononucleated cell, (b) Binucleated cell without micronuclei and (c) Binucleated cell with micronuclei.

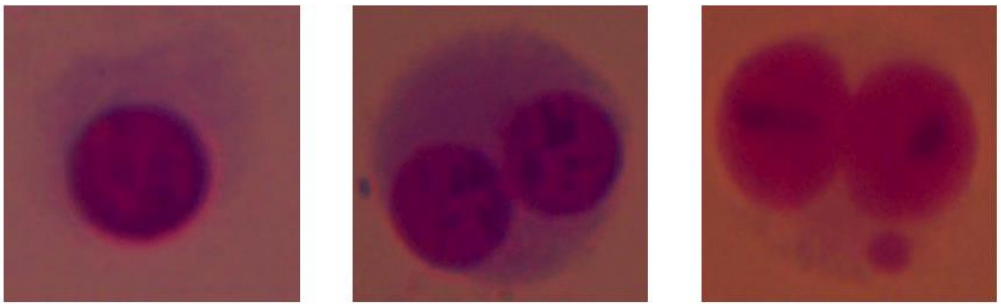

Fonte: Barbosa, 2026

The scope of our work is to identify the localization of binucleous cells without micronuclei (BN), binucleated cells with micronuclei (BNMN), and the micronuclei (MN) inside the binucleated cells. For the task, we aim to train a model 0, which receives as input a lymphocyte image and returns a set of bounding boxes and their associated classes $\theta(I) = \{(b_i, c_i) : b_i \in \mathbb{R}^4, c_i \in C, i = 1, \ldots, N\}$, where b_i denotes the i-th bounding box, c_i the corresponding class label, C = {BN, BNMN, MN} is the set of possible classes, and is the number of detected objects in the image.

4 METHODOLOGY

4.1 Dataset

The dataset used in this study was constructed using images of binucleated lymphocytes obtained directly from biological samples processed at the CRCN-NE laboratory. We call our built dataset MN-CRCN. The image capture was performed manually, under expert supervision, using a Leica DM 500 optical microscope with a resolution of 2048 x 1536 pixels.

To ensure the scientific quality and validity of the samples, the collected images were periodically reviewed and validated by experienced cytogeneticists at CRCN. Validation followed the guidelines of the HUMN (Human Micronucleus Project) [15], a widely recognized protocol in the scientific community for standardizing micronucleus analysis. The HUMN project establishes rigorous criteria for the analysis of binucleated cells, taking into account characteristics such as nuclear size, micronucleus size, and cytoplasmic integrity, among others.

According to these criteria, during the validation phase, some images were discarded for presenting irregularities such as overlapping nuclei, cytoplasmic damage, or poor contrast and focus quality. Figure 3 shows examples of images with annotations from MN-CRCN, containing images of the binucleated cells without micronucleus (BN), binucleated cells with micronucleus (BNMN) and micronucleus (MN) localization.

Figure 3 – Examples of images from MN-CRCN Dataset with annotated classes. Classes 0, 1 and 2 refer to nucleus cells without micronucleus, nucleus cells with micronucleus, and micronucleus localization, respectively.

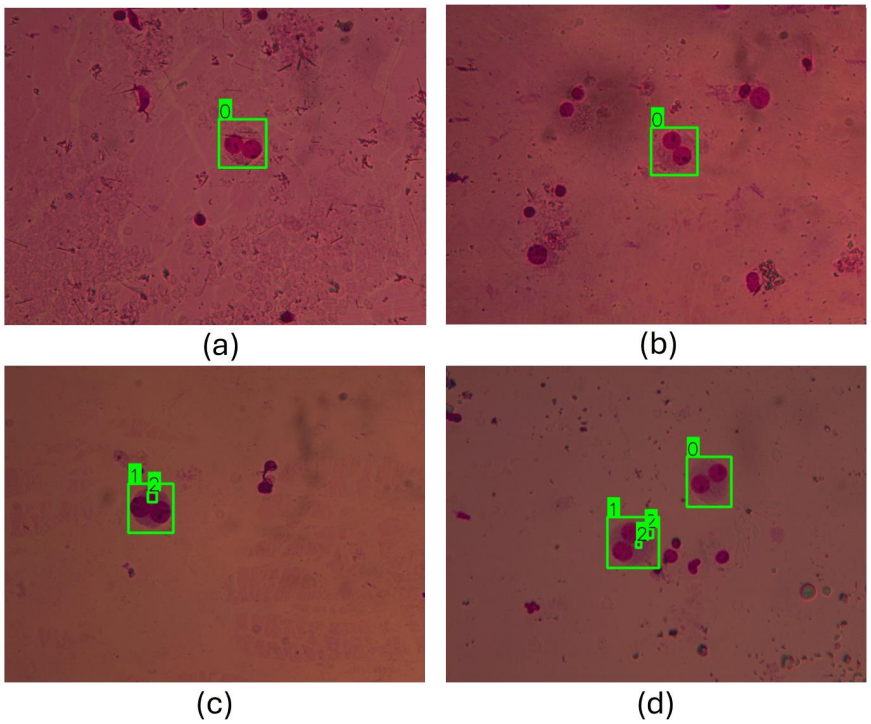

Fonte: Barbosa, 2026

A total of 889 captures were made, including 543 images of binucleated cells without micronuclei (BN) and 346 images of binucleated cells with micronuclei (BNMN). The images were originally captured in TIFF format and later converted to PNG. Table 1 presents the dataset statistics.

The dataset is split into training and test subsets, allocating 2/3 of the samples for training and 1/3 for testing, resulting in a training set of 621 images and a test set of 268 images

Table 1 – Distribution of the developed dataset. The second column shows the number of images containing each class, and the third column shows the total number of objects per class.

Class	No. of objects
Binucleated without micronucleus (BN)	600
Binucleated with micronucleus (BNMN)	347
Micronucleus (MN)	472
Total	1419

Fonte: Barbosa, 2026.

4.2 Implementation Details

We evaluated the SOTA models for object detection Faster-RCNN, FCOS, RetinaNet, YOLOv11, and YOLOv12. For all experiments, we resized the images to 1080 × 1080 pixels and trained for 200 epochs, with a learning rate of 0.001 and batch size of 8. These parameters were defined empirically, and the best results

were obtained. The experiments were conducted on Kaggle Notebook [16] using a V100 GPU.

YOLOv11 and YOLOv12 implementation was based on their public github code [3], [17]. We used YOLOv11m and YOLOv12m architectures pretrained on the COCO dataset [18] and fine-tuned it on our custom dataset.

Faster-RCNN, FCOS, and RetinaNet implementation were based on MMdetection github code [19]. We used ResNet-50 [20] as the backbone for Faster-RCNN, RetinaNet and FCOS. We used the default model parameters for each architecture, pretrained on the COCO dataset and using the same training parameters as YOLOv11 and YOLOv12.

4.3 Implementation Details

To evaluate the model's performance in the application, widely used metrics in computer vision were employed: *Mean Average Precision (mAP), Precision,* and *Recall*.

The Mean Average Precision (mAP) quantifies the overall model performance by computing the precision across different *IoU* (In-average tersection over Union) thresholds. We consider mAP50, which evaluates the model with a fixed IoU threshold of 0.50.

The Precision metric indicates the proportion of correct predictions relative to the total number of predictions made, serving as an indicator of the model's reliability. The formula for Precision is given by:

$$\mathrm{Pr}\,e\,cision = \frac{TP}{TP + FP'}$$

where TP and FP represent the number of true positives and false positives, respectively.

The Recall metric measures the proportion of actual classes correctly detected by the model. The formula for Recall is given by:

$$Recall = \frac{TP}{TP + FN}$$

5 RESULTS

We evaluated Faster-RCNN, FCOS, RetinaNet, YOLOv11, and YOLOv12 to the proposed MN-CRCN dataset. Table 2 shows the results of Precision, Recall and mAP50 metrics for each method and each class.

Figure 4 shows qualitative results of each method, where the green, red, and blue rectangles indicate true positives, false positives and false negatives, respectively.

Figure 4 – Detection results for Faster-RCNN, FCOS, RetinaNet, YOLOv11, and YOLOv12 on images from the MN-CRCN dataset. Bounding boxes in green, red and blue indicate true positives, false positives, and false negatives, respectively.

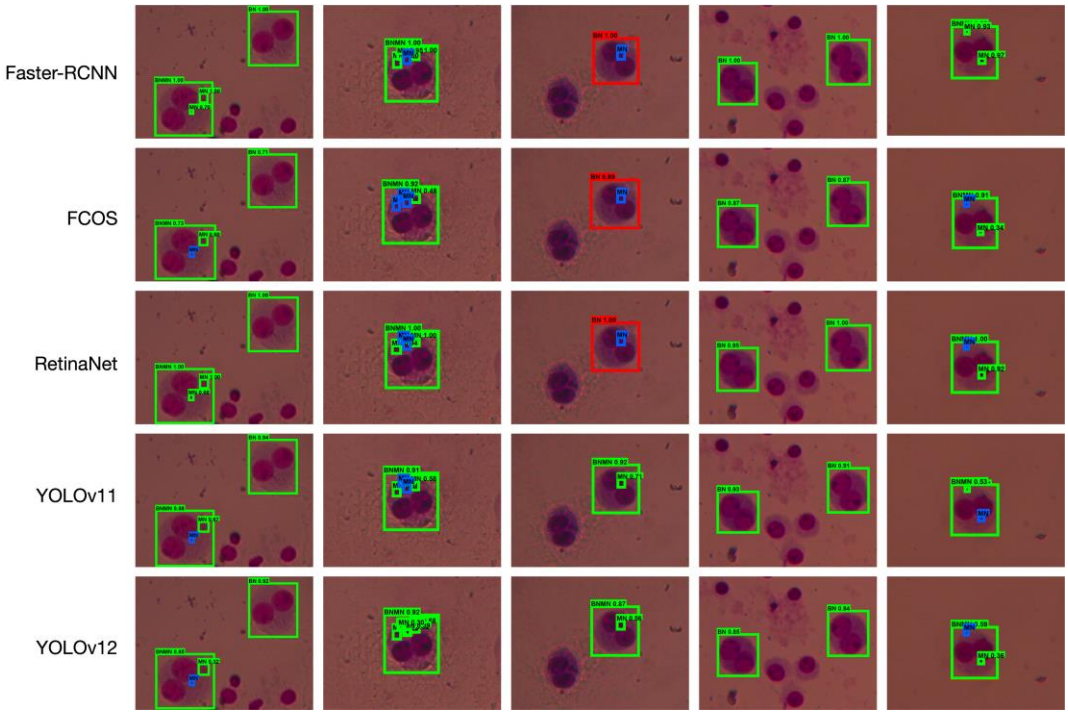

Fonte: Barbosa, 2026

From these examples, we observe that despite the presence of noise and other cells in the images, the model could identify the binucleated cells correctly. The model automatically ignored other cells because they were not binucleated or had atypical structures, such as nuclei of significantly different sizes, which were also excluded during annotation by the cytogeneticist. Table 2 show results of precision, recall and mAP50 for each method.

Table 2 – Results of precision, recall and mAP50 for the MN-CRCN dataset. Best values are presented in boldface.

Model	Class	Precision	Recall	mAP50
Faster-RCNN	BN	0.81	0.98	0.95
	BNMN	0.84	0.88	0.95
	MN	0.83	0.79	0.76
	All	0.83	0.88	0.88
FCOS	BN	0.81	0.98	0.91
	BNMN	0.85	0.81	0.89
	MN	0.78	0.64	0.26
	All	0.81	0.81	0.68
RetinaNet	BN	0.76	0.97	0.94
	BNMN	0.76	0.84	0.92
	MN	0.85	0.78	0.82
	All	0.79	0.86	0.89
YOLOv11	BN	0.88	0.99	0.97
	BNMN	0.93	0.99	0.98
	MN	0.95	0.80	0.93
	All	0.92	0.91	**0.96**

YOLOv12	BN	0.93	0.99	0.98
	BNMN	0.95	0.97	0.98
	MN	0.91	0.84	0.93
	All	**0.93**	**0.93**	**0.96**

Fonte: Barbosa, 2026.

Figure 5 shows the confusion matrix of each method. In the confusion matrix, BKND corresponds to the background and maps the false negative cases. We can observe that YOLOv12 obtained the best results, with fewer misclassifications. Most of the missing occurs in the MN class, as they are small and often classified as background.

Figure 5 – Confusion matrix os Faster-RCNN, FCOS, RetinaNet, YOLOv11, and YOLOv12, for MN-CRCN dataset

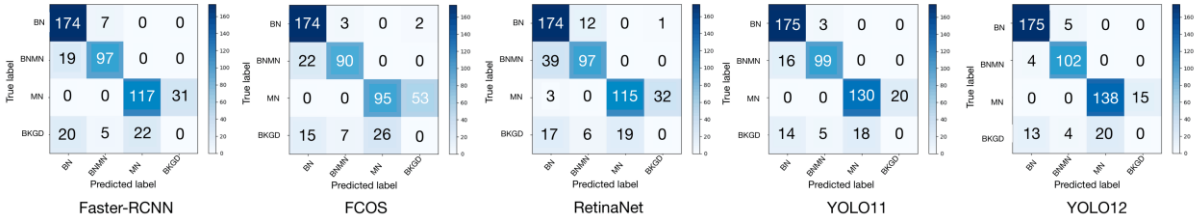

Fonte: Barbosa, 2026

6 CONCLUSION

In this work, we presented MN-CRCN, a new publicly available dataset for automatic detection of micronuclei in binucleated lymphocytes. The dataset, constructed using samples acquired and validated by expert cytogeneticists at CRCN-NE, includes detailed annotations of three biologically relevant classes: binucleated cells without micronuclei (BN), binucleated cells with micronuclei (BNMN), and isolated micronuclei (MN). We evaluated several state-of-the-art object detection models on the proposed dataset, including YOLOv11, YOLOv12, Faster R-CNN, RetinaNet, and FCOS. YOLOv11 achieved the best overall performance, with 93% precision, 93% recall, and 96% mAP@50, demonstrating its suitability for clinical and research applications. The MN-CRCN dataset addresses the current limitations of private datasets in the field and provides a reproducible benchmark for advancing automated micronucleus detection. Future work includes expanding the dataset and exploring models tailored for small object detection to improve the accuracy of micronucleus identification.

REFERÊNCIAS

[1] K. Krupina, A. Goginashvili, and D. W. Cleveland, "Causes and consequences of micronuclei," Current Opinion in Cell Biology, vol. 70, pp. 91-99, 2021, accessed: 2025-02-09. [Online]. Available: https: //www.sciencedirect.com/science/article/abs/pii/S0955067421000041

[2] P. Rohr, G. F. da Silva, V. E. P. Vicentini, I. V. de Almeida, R. A. Dos Santos, C. S. Takahashi, M. O. Goulart, G. N. da Silva, L. B. de Oliveira, C. K. Grisolia et al., "Buccal micronucleus cytome assay: Inter-laboratory scoring exercise and micronucleus and nuclear abnor-malities frequencies in different populations from brazil," Toxicology Letters, vol. 333, pp. 242-250, 2020.

[3] G. Jocher and J. Qiu, "Ultralytics yolo11," 2024. [Online]. Available: https://github.com/ultralytics/ultralytics

[4] H. Yoda, K. Abe, H. Takeo, T. Takamura-Enya, and A. Koike-Takeshita, "Application of image-recognition techniques to automated micronu-cleus detection in the in vitro micronucleus assay," Genes and Envi-ronment, vol. 46, no. 1, p. 11, 2024.

[5] A. Panchbhai, M. C. S. Ishanzadeh, A. Sidali, N. Solaiman, S. Pankanti, R. Kanagaraj, J. J. Murphy, and K. Surendranath, "A deep learning workflow for quantification of micronuclei in dna damage studies in cultured cancer cell lines: a proof of principle investigation," Computer Methods and Programs in Biomedicine, vol. 232, p. 107447, 2023.

[6] S. Ren, K. He, R. Girshick, and J. Sun, "Faster r-cnn: towards real-time object detection with region proposal networks," in Proceedings of the 29th International Conference on Neural Information Processing Systems - Volume 1, ser. NIPS' 15. Cambridge, MA, USA: MIT Press, 2015, p. 91-99.

[7] Z. Tian, C. Shen, H. Chen, and T. He, "Fcos: Fully convolutional one-stage object detection," in Proceedings of the IEEE/CVF international conference on computer vision, 2019, pp. 9627-9636.

[8] T.-Y. Lin, P. Goyal, R. Girshick, K. He, and P. Dollár, "Focal loss for dense object detection," in Proceedings of the IEEE international conference on computer vision, 2017, pp. 2980-2988.

[9] Y. Tian, Q. Ye, and D. Doermann, "Yolov12: Attention-centric real-time object detectors," 2025. [Online]. Available: https://github.com/sunsmarterjie/yolov12

[10] P. Jiang, D. Ergu, F. Liu, Y. Cai, and B. Ma, "A review of yolo algorithm developments," Procedia computer science, vol. 199, pp. 1066-1073, 2022.

[11] W. Wei, J. Li, X. Wu, and H. Zhang, "High-through cell micronucleus image detection method combining multi-attention mechanism and yolov5," Biomedical Signal Processing and Control, vol. 87, p. 105496, 2023, accessed: 2025-02-09. [Online]. Available: https://www.sciencedirect.com/science/article/pii/S1746809423004960

[12] W. Wei, Y. Leng, L. Cao et al., "Std-yolov7: A small target detector for micronucleus based on yolov7," 2024, accessed: 2025-02-09. [Online]. Available: https://papers.ssrn.com/sol3/papers.cfm?abstract_id=4844656

[13] M. A. Ibarra-Arellano, L. A. Caprio, A. Hada, N. Stotzem, L. Cai, S. Shah, J. C. Melms, F. Wünneman, B. Izar, and D. Schapiro, "micronuclai: Automated quantification of micronuclei for assessment of chromosomal instability," bioRxiv [Preprint), vol. 2024, no. 05.24.595722, 2024, accessed: 2025-02-09. [Online]. Available: https://doi.org/10.1101/2024.05.24.595722

[14] X. Shen, Y. Chen, C. Li et al., "Rapid and automatic detection of micronuclei in binucleated lymphocytes image," Scientific Reports, vol. 12, no. 1, 2022, accessed: 2025-02-09. [Online]. Available: https://www.nature.com/articles/s41598-022-07936-4

[15] M. Fenech, W. P. Chang, M. Kirsch-Volders et al., "Humn project: detailed description of the scoring criteria for the cytokinesis-block micronucleus assay using isolated human lymphocyte cultures," Mutation Research/Genetic Toxicology and Environmental Mutagenesis, vol. 534, no. 1-2, pp. 65-75, 2002, accessed: 2025-02-09. [Online]. Available: https://www.sciencedirect.com/science/article/abs/pii/S1383571802002498

[16] Kaggle, "Kaggle notebooks," 2025, url:https://www.kaggle.com/code. Acessado em: 20/02/2025. [Online]. Available: https://www.kaggle.com/code

[17] Y. Tian, Q. Ye, and D. Doermann, "Yolov12: Attention-centric real-time object detectors," arXiv preprint arXiv:2502.12524, 2025.

[18] S. Jain, S. Dash, R. Deorari et al., "Object detection using coco dataset," in 2022 International Conference on Cyber Resilience (ICCR). IEEE, 2022, pp. 1-4.

[19] K. Chen, J. Wang, J. Pang, Y. Cao, Y. Xiong, X. Li, S. Sun, W. Feng, Z. Liu, J. Xu, Z. Zhang, D. Cheng, C. Zhu, T. Cheng, Q. Zhao, B. Li, X. Lu, R. Zhu, Y. Wu, J. Dai, J. Wang, J. Shi, W. Ouyang, C. C. Loy, and D. Lin, "MMDetection: Open mmlab detection toolbox and benchmark," arXiv preprint arXiv:1906.07155, 2019.

[20] K. He, X. Zhang, S. Ren, and J. Sun, "Deep residual learning for image recognition," in Proceedings of the IEEE conference on computer vision and pattern recognition, 2016, pp. 770-778.